Composite Structures 108 (2014) 65–76

Contents lists available at ScienceDirect

Composite Structures

journal homepage: www.elsevier.com/locate/compstruct

Optimal design of rectangular composite flat-panel sound radiators considering excitation location

C.H. Jiang, Y.H. Chang, T.Y. Kam *

Mechanical Engineering Department, National Chiao Tung University, Hsin Chu 300, Taiwan

ARTICLE INFO

Article history:
Available online 14 September 2013

Keywords:
Acoustics
Composite plate
Optimal design
Rayleigh–Ritz method
Sound radiation

ABSTRACT

The optimal excitation locations of rectangular composite sound radiation plates to produce relatively smooth sound level pressure (SPL) curves are determined using an optimal design method. In the optimal design process, the vibration of the plate is analyzed using the Rayleigh–Ritz method, the sound pressure produced by the plate is calculated using the first Rayleigh integral, and the optimal excitation location is determined using a global optimization technique. The experimental SPL curves of several sound radiators were measured to verify the accuracy of the theoretical predictions. In the determination of the optimal excitation location, the trial radius of the circular excitation force is used in the vibro-acoustic analysis to predict the theoretical SPL curve of the plate, a SPL discrepancy function is established to measure the sum of the squared differences between the SPLs at the chosen excitation frequencies and the average value of such SPLs, and a global minimization technique is used to search for the best estimate of the radius of the circular excitation force by making the SPL discrepancy function a global minimum. The optimal excitation locations of several composite sound radiators with different aspect ratios and layups are determined using the proposed method.

1. Introduction

The advantages of composite materials such as high stiffness-to-weight and strength-to-weight ratios have made composite plates find broad applications in different industries such as aero-space, aircraft, automobile, and audio industries to fabricate structures of high performance and reliability. In general, the design of composite plate structures has to tackle the structural vibro-acoustic issue to achieve the goals and functions of these structures. For instance, in the audio industry, composite plates have been used to fabricate composite panel-form sound radiators or speakers for sound radiation. For a panel-form sound radiator/speaker, the sound radiation is induced by the vibration of the plate which is flexibly restrained at its edges and excited by at least one exciter. Therefore, the vibro-acoustics of composite plates has become an important topic of research in the design of composite flat-panel speakers for achieving high quality sound radiation of the speakers. Recently, several researchers have proposed different types of composite panel-form sound radiators [1–7] which may find applications in the consumer electronics. For instance, Guenther and Leigh [1] proposed the use of a composite sandwich sound radiation plate comprising carbon fiber reinforced face sheets and honeycomb core in a flat-panel speaker for attaining improved performance at higher frequencies. Kam [6] proposed the use of a plural number of exciters to excite the composite plate of a panel-form sound radiator at some specific locations to produce a smooth SPL curve for the sound radiator. Since the sound radiation efficiency and quality of a plate are heavily dependent of the vibration characteristics of the plate, the vibro-acoustics of plate structures has thus been studied by many researchers. For instance, many papers [8–20] have been devoted to the vibration and/or sound radiation analyses of plates with different boundary conditions and structural configurations subjected to various types of loads. A number of researchers [21–23] have studied the effects of attached masses on the sound radiation behaviors of plates with regular or flexibly restrained boundary conditions. Regarding the effects of loading conditions on the sound radiation capability of plates, several researchers have studied the SPL curves of plates subjected to different types of loads and excited at various locations [24,25]. As for composite flat-panel sound radiators consisting of one exciter, which may find important applications in the audio industry, no work has been devoted to study how the excitation location affect the sound quality of such sound radiators, not to mention the determination of the optimal excitation locations for the sound radiators. Therefore, the sound radiation behavior of composite flat-panel sound radiation deserves a thorough investigation if flat-panel speakers with good sound quality are to be fabricated.

In this paper, an optimal design method is proposed to determine the optimal excitation locations for composite panel-form

* Corresponding author. Fax: +886 3 6125057.
E-mail address: tykam@mail.nctu.edu.tw (T.Y. Kam).

0263-8223/$ - see front matter © 2013 Elsevier Ltd. All rights reserved.
http://dx.doi.org/10.1016/j.compstruct.2013.09.005

sound radiators consisting of one exciter to possess relatively smooth SPL curves. The vibro-acoustics, especially, the SPL curves of composite panel-form sound radiators are studied via both theoretical and experimental approaches. The Rayleigh–Ritz method together with the first Rayleigh integral is used to study the vibro-acoustic behaviors and construct the SPL curves of the composite plates. The theoretically predicted SPL curves will be verified by the experimental results obtained in this paper. The optimal excitation locations of various sound radiators are determined to produce relatively smooth SPL curves in the given frequency ranges.

2. Plate vibration analysis

In this study, a flat-panel sound radiator consisting of a center exciter is mathematically modeled as an elastically restrained stiffened plate. The stiffened rectangular composite plate of size a (length) $\times$ b (width) $\times$ h_p (thickness) with $a \geqq b$ is elastically restrained along the plate periphery by distributed springs with translational and rotational spring constant intensities K_{Li} and K_{Ri}, respectively, and at the center by a spring of spring constant K_c as shown in Fig. 1. The x–y plane of the global x–y–z coordinate is located at the mid-plane of the symmetrically laminated composite plate which consists of NL orthotropic laminae having different fiber angles with reference to the x-axis. It is noted that the plate is stiffened symmetrically in x and y directions by a number of beams on the bottom surface of the plate. Herein, the displacements of the plate and stiffeners are modeled based on the first-order shear deformation theory [26]. The displacement field of the plate is expressed as

$$\begin{aligned} u_p &= u_{op}(x,y,t) - z_p\theta_{xp}(x,y,t) \\ v_p &= v_{op}(x,y,t) - z_p\theta_{yp}(x,y,t) \\ w_p &= w_{op}(x,y,t) \end{aligned} \tag{1}$$

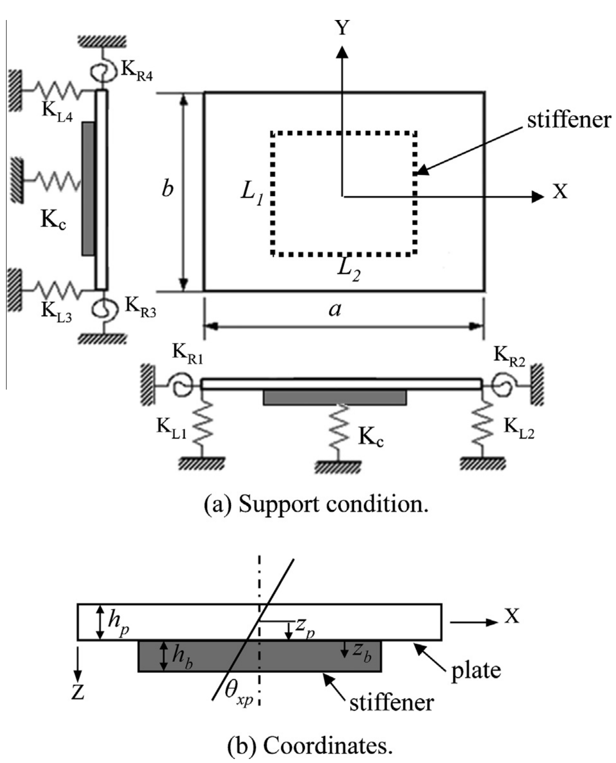

Fig. 1. Elastically restrained stiffened plate.

where u_p, v_p, and w_p are the displacements in x, y, and z directions, respectively; u_{op}, v_{op}, w_{op} are mid-plane displacements; θ_{xp}, θ_{yp} are shear rotations. It is assumed that both the plate and stiffeners have the same shear rotations. The strain–displacement relations of the plate are expressed as

$$\begin{aligned} \varepsilon_x &= \frac{\partial u}{\partial x} = \frac{\partial u_{op}}{\partial x} + z_p\frac{\partial \theta_{xp}}{\partial x} \\ \varepsilon_y &= \frac{\partial v}{\partial y} = \frac{\partial v_{op}}{\partial y} + z_p\frac{\partial \theta_{yp}}{\partial y} \\ \varepsilon_z &= \frac{\partial w}{\partial z} = \frac{\partial w_{op}}{\partial y} = 0 \\ \gamma_{yz} &= \frac{\partial v}{\partial z} + \frac{\partial w}{\partial y} = \theta_{yp} + \frac{\partial w_{op}}{\partial y} \\ \gamma_{xz} &= \frac{\partial u}{\partial z} + \frac{\partial w}{\partial y} = \theta_{xp} + \frac{\partial w_{op}}{\partial x} \\ \gamma_{xy} &= \frac{\partial u}{\partial y} + \frac{\partial v}{\partial x} = \left(\frac{\partial u_{op}}{\partial y} + \frac{\partial v_{op}}{\partial x}\right) + z_p\left(\frac{\partial \theta_{xp}}{\partial y} + \frac{\partial \theta_{yp}}{\partial x}\right) \end{aligned} \tag{2}$$

The stress–strain relations for the layers in the global x–y–z coordinate system can be expressed in the following general form [27].

$$\begin{Bmatrix} \sigma_x^{(k)} \\ \sigma_y^{(k)} \\ \sigma_z^{(k)} \\ \tau_{yz}^{(k)} \\ \tau_{xz}^{(k)} \\ \tau_{xy}^{(k)} \end{Bmatrix} = \begin{bmatrix} \overline{Q}_{11}^{(k)} & \overline{Q}_{12}^{(k)} & \overline{Q}_{16}^{(k)} & 0 & 0 \\ \overline{Q}_{12}^{(k)} & \overline{Q}_{22}^{(k)} & \overline{Q}_{26}^{(k)} & 0 & 0 \\ \overline{Q}_{16}^{(k)} & \overline{Q}_{26}^{(k)} & \overline{Q}_{66}^{(k)} & 0 & 0 \\ 0 & 0 & 0 & \overline{Q}_{44}^{(k)} & \overline{Q}_{45}^{(k)} \\ 0 & 0 & 0 & \overline{Q}_{45}^{(k)} & \overline{Q}_{55}^{(k)} \end{bmatrix} \cdot \begin{Bmatrix} \varepsilon_x^{(k)} \\ \varepsilon_y^{(k)} \\ \varepsilon_z^{(k)} \\ \gamma_{yz}^{(k)} \\ \gamma_{xz}^{(k)} \\ \gamma_{xy}^{(k)} \end{Bmatrix} \tag{3}$$

where σ, τ are normal and shear stresses, respectively; $\overline{Q}_{ij}^{(k)}$ are the transformed lamina stiffness coefficients which depend on the material properties and fiber orientation of the kth lamina. The relations between the transformed and untransformed lamina stiffness coefficients are expressed as

$$\begin{aligned} \overline{Q}_{11} &= Q_{11}C^4 + 2(Q_{12} + 2Q_{66})C^2S^2 + Q_{22}S^4 \\ \overline{Q}_{12} &= (Q_{11} + Q_{22} - 4Q_{66})C^2S^2 + Q_{12}(C^4 + S^4) \\ \overline{Q}_{16} &= (Q_{11} - Q_{12} - 2Q_{66})C^3S + (Q_{12} - Q_{22} + 2Q_{66})CS^3 \\ \overline{Q}_{22} &= Q_{11}S^4 + 2(Q_{12} + 2Q_{66})C^2S^2 + Q_{22}C^4 \\ \overline{Q}_{26} &= (Q_{11} - Q_{12} - 2Q_{66})CS^3 + (Q_{12} - Q_{22} + 2Q_{66})C^3S \\ \overline{Q}_{66} &= (Q_{11} + Q_{22} - 2Q_{12} - 2Q_{66})C^2S^2 + Q_{66}(C^4 + S^4) \\ \overline{Q}_{44} &= Q_{44}C^2 + Q_{55}S^2, \overline{Q}_{45} = (Q_{55} - Q_{44})CS \\ \overline{Q}_{55} &= Q_{55}C^2 + Q_{44}S^2 \end{aligned} \tag{4a}$$

with

$$\begin{aligned} &Q_{11} = \frac{E_1}{1 - V_{12}V_{21}}; \quad Q_{12} = \frac{V_{12}E_2}{1 - V_{12}V_{21}}; \quad Q_{22} = \frac{E_2}{1 - V_{12}V_{21}} \\ &Q_{44} = G_{23}; \quad Q_{55} = G_{13}; \quad Q_{66} = G_{12}; \quad C = \cos\theta_i, \quad S = \sin\theta_i \end{aligned} \tag{4b}$$

where Q_{ij} are untransformed lamina stiffness coefficients; E_1, E_2 are Young's moduli in the fiber and transverse directions, respectively; V_{ij} is Poisson's ratio for transverse strain in the j-direction when stressed in the i-direction; G_{12} is in-plane shear modulus in the 1–2 plane; G_{12} G_{23} and are transverse shear moduli in the 1–3 and 2–3 planes, respectively; θ_i is the lamina fiber angle of the ith lamina.

The strain energy, U_p, of the plate with volume V_p is

$$U_p = \frac{1}{2}\int_{V_p} (\sigma_x\varepsilon_x + \sigma_y\varepsilon_y + \tau_{xy}\gamma_{xy} + \tau_{xz}\gamma_{xz} + \tau_{zy}\gamma_{zy})dV_p \tag{5}$$

Using the relations in Eqs. (1)–(4) and integrating through the plate thickness, Eq. (5) can be rewritten as